Research Article

Sathyanarayana Srinivas, Hattinaik Hema, Devalapura Chikkakalaiah Madaiah, Rajashekaraiah Hemanth, Bheemappa Suresha*, Irulappasamy Siva, Sharul Sham Dol, Kamarul Arifin Ahmad and Mohamed Thariq Hameed Sultan*

Dual nanofiller strategy for enhanced mechanical properties in carbon fiber reinforced polyamide blends

https://doi.org/10.1515/ntrev-2025-0235
Received May 3, 2025; accepted September 30, 2025;
published online January 8, 2026

Abstract: The polyamide/thermoplastic copolyester (PA/CoPe) blend is unique among the limited selection of thermoplastic matrices due to its enhanced mechanical and physical characteristics. Exploring the sway of silane-treated silica and graphene nanofillers on the mechanical behavior of short carbon fiber/PA6/CoPe blend (CF/PA blend) composites is the central aim of this work. Two distinct nanocomposites were made by extrusion and injection molding. The first incorporated silica nanofillers, while the second used a combination of graphene and silica. Hardness, tensile, short beam, flexure, and impact tests were performed to ascertain the effect of the nanofillers on mechanical behavior. Experimentally, nanofillers noticeably improved the composite's mechanical properties, with silane treatment fostering superior nanofiller-matrix bonding. The synergistic effect of silica and graphene led to a significant 32.3 % increase in interlaminar shear strength. Moreover, this combination yielded substantial gains in hardness (14.1 %), tensile strength (16 %), flexural strength (19 %), and impact strength (33.2 %) over the unfilled blend. Conversely, using 1.5 % silica as the sole reinforcement resulted in smaller increases of 8.5 %, 5.6 %, 5.4 %, and 8.5 % for the same mechanical attributes. Together, these nanofillers improve network structure formation and silica and graphene dispersion, strengthening the CF/PA blend composite's mechanical characteristics. Additionally, this will open the door to creative structural engineering designs and more environmentally friendly solutions.

Keywords: CF/PA blend composite; nanofillers; silane treatment; mechanical properties; fractography

***Corresponding authors: Bheemappa Suresha**, Department of Polymer Science and Technology, JSS Science and Technology University, Mysuru, 570006, Karnataka, India; and Department of Mechanical Engineering, JSS Science and Technology University, Mysuru, 570006, Karnataka, India, E-mail: suresha.b2005@gmail.com; and **Mohamed Thariq Hameed Sultan**, Department of Aerospace Engineering, Faculty of Engineering, Universiti Putra Malaysia, 43400, Serdang, Selangor, Malaysia; Laboratory of Biocomposite Technology, Institute of Tropical Forest and Forest Product (INTROP), Universiti Putra Malaysia, 43400 UPM, Serdang, Selangor, Malaysia; and Aerospace Malaysia Innovation Centre [944751-A], Prime Minister's Department, MIGHT Partnership Hub, Jalan Impact, 63600, Cyberjaya, Selangor, Malaysia, E-mail: thariq@upm.edu.my. https://orcid.org/0000-0002-5110-0242
Sathyanarayana Srinivas, Department of Polymer Science and Technology, JSS Science and Technology University, Mysuru, 570006, Karnataka, India, E-mail: srinivas.sathyanarayana@gmail.com
Hattinaik Hema and Rajashekaraiah Hemanth, Department of Civil Engineering, The National Institute of Engineering, Mysuru, 570008, Karnataka, India, E-mail: hemah@nie.ac.in (H. Hema), hemanthr@nie.ac.in (R. Hemanth). https://orcid.org/0000-0003-4805-6057 (H. Hema)
Devalapura Chikkakalaiah Madaiah, Department of Mechanical Engineering, JSS Science and Technology University, Mysuru, 570006, Karnataka, India, E-mail: madaiahdc@nie.ac.in
Irulappasamy Siva, Department of Mechanical Engineering, Mohan babu University, Tirupati, 517101, Andhra Pradesh, India, E-mail: drisivamech@gmail.com
Sharul Sham Dol, Department Mechanical and Industrial Engineering, Abu Dhabi University, PO Box 59911, Abu Dhabi, United Arab Emirates. https://orcid.org/0000-0001-6324-6217
Kamarul Arifin Ahmad, Department of Aerospace Engineering, Faculty of Engineering, Universiti Putra Malaysia, 43400, Serdang, Selangor, Malaysia

Highlights

- Multiscale composites were developed by integrating fibers and nanomaterials.
- Uniform dispersion in the polymer blend is essential for enhanced properties.
- Composites gained significant mechanical strength.
- Silane treatment strengthened filler-matrix interface.
- Synergic effect of carbon fiber and nanofillers was demonstrated.
- Properties meet automotive and aerospace performance requirements.

1 Introduction

Functional nanometer-sized fillers are now crucial for reinforcing polymeric composite materials. Over the past two decades, there has been a lot of interest in nano-level fillers like silicon dioxide and layered graphene that form nanostructures with polymers [1–4]. Because of their large surface area, which improves load transfer within the polymer matrix and strengthens the interfacial bonding, these nanofillers significantly improve the mechanical performance of thermoplastics (TPs), particularly in harsh environments like high temperatures and ultraviolet (UV) radiation. By combining graphene nanoplatelets (GNPs) and FeO_4 nanoparticles, Şenyurt et al. [5] created PAN nanofiber-reinforced Elium® composites that simultaneously improved mechanical performance, thermal stability, and shape memory behavior. The dual-doped system was positioned as a promising contender for advanced engineering applications due to its evident synergistic effects. Elium®-based thermoplastic nanocomposites reinforced with PAN nanofibers doped with Ag and SiC nanoparticles were created by Kurdis et al. [6], who achieved notable gains in X-ray attenuation, thermal stability, and tensile strength. These lightweight, recyclable composites are prospective substitutes for radiation-shielding applications in aircraft, defense, and medicine due to their multifunctional functionality. Furthermore, as demonstrated by TiO_2 nanoparticles improving the mechanical properties of polyethylene [7], nanofillers can lessen the effects of degradation. Similarly, Danbee Lee et al. [8] showed that the mechanical properties and weathering resistance of polypropylene composites are significantly enhanced by the combination of talc fillers, UV stabilizers, and nano-calcium carbonate (n-$CaCO_3$).

In carbon fiber-reinforced thermoplastic composites, Yuan et al. [9] pointed out that the surface characteristics of the carbon fibers and the polymer matrix's capacity for melt infiltration have a critical impact on the interface performance. Polarity differences between matrices have a major impact on interfacial bonding and overall mechanical properties. A new carbon fiber composite mechanical metamaterial with both multi-stable and mono-stable properties was developed by Sun et al. [10] and verified using finite element modeling and quasi-static compression tests. Their findings highlight its potential for impact energy absorption and vibration attenuation applications by demonstrating that higher torque is needed to move from mono-stable to multi-stable states. Also, using carbon fiber composites and hot-pressing and discrete assembly, Sun et al. [11] developed a mechanical metamaterial with both multi-stable and mono-stable properties. A modular torsion inhibition technique enhanced stability, and simulations closely matched experiments, demonstrating the material's potential for energy absorption and vibration damping. In comparison to virgin carbon fibers, Shi et al. [12] found that recycled carbon fibers greatly improve the cement mortar's fracture toughness, ductility, and fracture energy while lowering its environmental impact, demonstrating the sustainability and engineering viability of these fibers. A bio-inspired hexagonal-quadrilateral lattice structure (HQLS) was introduced by Yang et al. [13] inside steel/CFRP hybrid tubes, greatly enhancing mechanical performance and energy absorption. Their experimentally validated model has a lot of potential for use in rail vehicle crashworthiness applications. To precisely forecast the mechanical behavior of carbon fiber reinforced polymers with voids, Yao et al. [14] used 3D computed tomography in conjunction with multi-scale homogenization modeling. They found that direction-dependent modulus weakening is caused by void distribution and morphology. Thus, using the synergistic effects of combined nanofillers, the current study expands on this foundation by examining a dual nanofiller strategy to improve the mechanical properties of carbon fiber reinforced polyamide blends.

Nylon 6, also known as polyamide 6 (PA 6), is a multipurpose thermoplastic that is well-known for its exceptional blend of mechanical performance, processability, and affordability [15]. While its elasticity and impact resistance allow it to absorb vibrations and shocks in dynamic applications, its high tensile strength, toughness, and abrasion resistance make it perfect for load-bearing components like gears, bearings, and structural parts [16, 17]. Furthermore, PA 6 is a popular choice in a variety of engineering sectors, such as consumer goods, industrial machinery, and automotive, due to its balanced mechanical properties and ease of processing through methods like injection molding and extrusion [18]. Mechanical properties are further enhanced by PA 6 through multilayers with functional nanofillers and complementary elastomeric blends [19–21]. Furthermore, carbon fiber reinforcement results in advanced composites (CF/PA), which are prized for their lightweight and economic performance in the marine, automotive, and aerospace industries [22, 23].

Currently, polymer blends make up more than 30 % of all polymer consumption, and their potential to produce high-performance, reasonably priced materials is expected to drive their 9 % annual growth rate [22]. By creating covalent bonds with functional groups in polymers or fillers and promoting interfacial adhesion through graft or block copolymer formation at the interface, maleic anhydride-grafted compatibilizers play a crucial role in improving mechanical properties such as tensile strength and elongation at break [24–29].

For automotive and marine applications, glass fibers (GFs) and carbon fibers (CFs) are two of the most popular reinforcements in polymer matrices. Because of their high energy absorption, recyclability, and promise for building lightweight, fuel-efficient buildings, thermoplastic composites have drawn more attention in recent years. Elium®, a thermoplastic resin based on acrylic, is notable among them for its capacity to improve stiffness and toughness [30]. Its significant promise for durable and damage-tolerant applications is further demonstrated by the fact that it makes it possible to create curable but non-permanent adhesive junctions that have better mechanical strength and load-bearing capacity than traditional epoxy systems [31]. GFs are more affordable and provide good strength, stiffness, and superior impact resistance because of their deformability under stress [32]. According to Mostafa et al.'s [33] research, residual stress within the constituents are influenced by both the composite's elastic properties and fiber pretension. On the other hand, CFs offer greater stiffness and tensile strength, are lighter, and enhance fuel efficiency in structures; however, their expense may raise the total cost of the composite [34]. Whereas CFs show greater tensile strengths ranging from 800 to 1,000 MPa for composites and approximately 4,137 MPa for fibers, but lower impact resistance because of brittleness, GFs show tensile strengths of roughly 3,450 MPa for fibers and 460 MPa for composites [35]. Thus, because of their resilience and capacity to absorb energy, GF-reinforced composites perform exceptionally well in impact-critical applications [36].

The type, loading, size, surface area, and compatibility of the reinforcing fibers and nanoparticles within the polymer matrix all affect the performance of fiber-reinforced polymer nanocomposites. To improve stiffness, hardness, and strength, a variety of nanofillers are utilized, including graphite nanoplatelets (Gnps) [37], graphene oxide (GO) [38], carbon nanotubes (Cnts) [39], nano-SiO_2 [40–42], and cellulose nanofibers [43]. Microscale fibers, such as carbon fibers (CFs) and glass fibers (GFs) [44], are also utilized. By combining GO, Cnts, and CFs through *in situ* interfacial polymerization [45], hybrid PA-based composites exhibit improved mechanical properties and optimized interphases.

Recently, researchers have investigated the mechanical, thermal, dimensional, and flame-retardant properties of nano-SiO_2 as effective reinfrocements [46, 47]. Cnts increase stiffness and tensile strength but are hydrophobic and require surface functionalization [48]. In contrast, GO's hydrophilic groups improve dispersion and adhesion in PA, which results in improved mechanical performance [49]. The effects of both fillers on thermal stability vary depending on the PA matrix and reduction level [50, 51]; however, Cnts generally enhance the thermal stability of polyamide composites [52, 53]. As a result, GO provides superior dispersion and compatibility in PA composites, while Cnts increase mechanical strength and electrical conductivity, thereby bolstering a dual nanofiller approach for improved composite performance [54, 55].

Surface-modified nano-SiO_2 significantly enhances the mechanical properties and dimensional stability of polymer composites by reducing thermal expansion and improving dispersion. Their high surface area and aspect ratio boost modulus, toughness, and tensile strength, while strong interactions with polymer chains improve load transfer and adhesion. Silane coupling agents have been developed to further strengthen filler–matrix bonding [56–58]. By reacting with both the filler and the matrix, these agents' dual functional groups strengthen the interface by forming chemical bridges [59]. The strong bonding improves mechanical properties such as impact resistance and tensile strength [60, 61]. Better filler dispersion within the polymer is encouraged by this improved wettability, creating a more homogeneous composite material and improving load transfer efficiency [62]. By adding short fibers and micro-scale fillers as reinforcements, Hemanth et al. [63] sought to improve the mechanical characteristics of TP Copolyester elastomer/polytetrafluoroethylene (TCE/PTFE) composites. The composite's tensile modulus, flexural strength, and impact resistance were all markedly enhanced by the addition of 20 % GFs. Behera et al. [64] observed a negative effect with graphene nanoplatelets and reported 34 %, 88 %, and 87 % increases in Young's modulus, flexural modulus, and impact strength, respectively, for a PBAT/HDPE blend with 3 phr Cnts in comparison to the neat blend. Umesh et al. [65] discovered that while adding Gnps to PA66/PA6 micro-composites greatly increased flexural strength at the expense of impact strength, it also slightly decreased tensile strength due to decreased ductility. Suresha et al. [32] studied the mechanical properties of PA66/TCE blend reinforced with CFs and filled with Gnps. They reported that the inclusion of CFs has significantly improved the tensile, flexural and impact properties of the PA66/TCE blend. Durmaz and Aytac [66] investigated the combined effects of micro- and nano-fillers on the performance of PA 11/PLA blends, focusing on their mechanical and thermo-mechanical properties. By adding TiB_2 and B_4C ceramic fillers to lightweight phenolic aerogel/carbon fiber composites, Liu et al. [67] were able to achieve exceptional thermal stability, oxidation resistance, and ablation resistance that makes them appropriate for hypersonic vehicle thermal protection. The composites' exceptional strength, low thermal conductivity, and resilience to harsh environments were made possible by the synergistic high-temperature ceramic reactions and multiphase ceramic structures. In their investigation of PA6/high-density polyethylene (HDPE)/carbon black (CB) composites, Wang et al. [68] found that a 4.5 %

CB content enhanced the composites' tensile strength to 53.3 MPa and impact strength to 13.2 J/m^2. This was possible because of the uniform dispersion of CB, which improved stress distribution and impact absorption. These findings highlight the vital role nanofillers play in enhancing hybrid TP composites' performance and adaptability, thereby increasing their potential industrial applications.

Nanofillers like Gnps and nano-SiO_2 play a crucial role in balancing ductility and mechanical performance in polymer matrices. The high surface area and reactivity of n-SiO_2 enhance stiffness, tensile strength, and load transfer through strong interfacial bonding, while Gnps significantly improve stiffness and strength when well-dispersed, though their rigidity may reduce ductility by limiting polymer chain mobility. Mechanical improvements depend on dispersion, interfacial interaction, and Gnps content [66, 69].

Studies assessing the mechanical performance of hybrid nanocomposites comprising silane-treated silica and graphene nanofillers and carbon fiber-reinforced polyamide with thermoplastic Copolyester (CoPe) are lacking, which represents a research gap. Investigating a dual nanofiller approach to improve impact and tensile fracture behavior in CF/PA blends is what makes this study novel. One aspect of the scope is comprehending the synergistic strengthening mechanisms that combined nanofillers offer in load-bearing applications, especially in the machinery and automotive industries. Potential final uses include the fabrication of sophisticated hybrid thermoplastic composites for high-performance and structural applications that have exceptional mechanical and durability characteristics.

2 Experimental section

2.1 Materials

Commercially available polyamide 6 (PA6; Gujlon E-28, 2.8 RV) from Gujarat State Fertilizer Corporation, Surat, India, and TP co-polyester (CoPe), TPC-ET, Arnitel EL-740 from DSM India were used. Short carbon fibers (CFs) from Toray were employed in this study. We purchased graphene Nano sheets (750 m^2 g^{-1} surface area, 3–6 layers, 50 nm thick) and aminopropyltriethoxy silane-treated nano-silica (10–20 nm) from Sigma Aldrich in Bangalore, India. According to the manufacturer, the silica powder has a density of 2.2–2.6 g cm^{-3} at 25 °C. The density of graphene is between 0.2 and 0.4 g cm^{-3}.

2.2 Preparation of composites

As shown in Figure 1, the first step for producing CF/PA blend composites is to dry mix PA 6, CoPe, and ethylene glycol pellets in a drum tumbler mixing machine for 10 min to ensure uniform component blending. A twin-screw co-rotating extruder (Krauss Maffei ZE24 mm) is then fed this well combined mixture at a feed rate of 30 kg h^{-1}. Extruded strands of 3 mm diameter are produced by melting and homogenizing the mixture inside the extruder, which has 11 zones and a 5-hole die, at 240 °C across the barrel and 250 °C at the die exit. The screw speed is 400 rpm, and the torque is 70 Nm.

The hot extrudate strands are pelletized into 3.5 mm granules after being quenched in a cold-water bath. To improve molding consistency and eliminate surface moisture, these composite granules are preheated for 3 h at 80 °C. Test specimens are then produced by processing the dried pellets in a reciprocating screw injection molding machine. For better moisture resistance, the PA blend ratio is kept at 80:20 (PA6: CoPe), producing PA6 as the continuous phase and CoPe as the dispersed phase. 25 wt% carbon fiber-reinforced PA blends (H0) are made for the composite formulation, and specific amounts of graphene and silica are added to create hybrid nanocomposites (H1, H2, H3); each composition is accurately listed in Table 1.

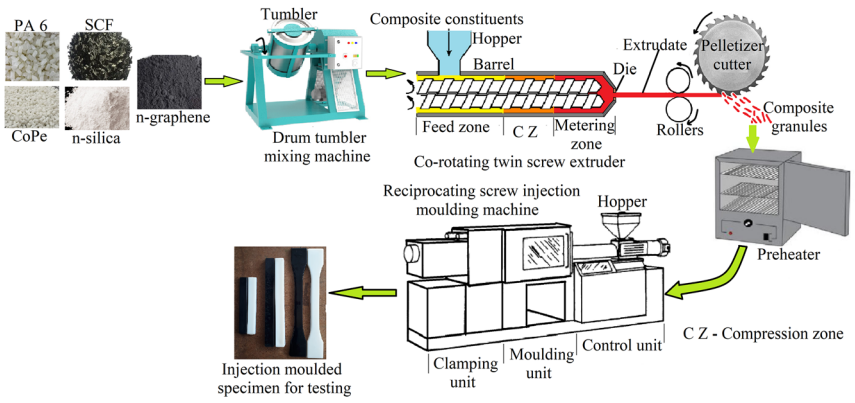

Figure 1: Process flow for creating CF/PA blends and their composites.

Table 1: List of nanocomposites produced in this work.

Composites	Designation	Composition (wt.%)
CF/PA + CoPe	H0	CF (25)/PA (60) + CoPe (15)
CF/PA + CoPe/silica	H1	CF (25)/PA (59.25) + CoPe (15)/Silica (0.75)
CF/PA + CoPe/silica	H2	CF (25)/PA (58.50) + CoPe (15)/Silica (1.50)
CF/PA + CoPe/silica + graphene	H3	CF (25)/PA (59.25) + CoPe (15)/Silica (0.75) + graphene (0.75)

As shown by the prepared specimens in Figure 2, the resulting injection-molded composites are then used for mechanical testing. Consistent specimen quality is appropriate for assessing composite mechanical performance, optimal interfacial bonding, and uniform filler dispersion is ensured by this methodical procedure.

2.3 Testing of hybrid nanocomposites

2.3.1 Density measurement

An Archimedes' principle-based densitometer determined the density of H0 and its hybrid nanocomposite samples (H1, H2, and H3). Equation (1) calculated the actual density, with each data point representing the average of three tests.

$$\rho_a = \frac{\rho_w \times W_a}{(W_a - W_w)} \tag{1}$$

where ρ_a = measured density, ρ_w = density of water, W_a = weight of the sample in air, W_w = weight of the sample in the water.

Agarwal and Broutman's formula (2) used to calculate the composite material's theoretical density (ρ_t) [70].

$$\rho_t = \frac{1}{\left(\frac{w_f}{\rho_f}\right) + \left(\frac{w_s}{\rho_s}\right) + \left(\frac{w_g}{\rho_g}\right) + \left(\frac{w_m}{\rho_m}\right)} \tag{2}$$

where w_f = weight fraction of CFs, w_s = weight fraction of silica, w_g = weight fraction of graphene, w_m = weight fraction of matrix, ρ_f = density of carbon fiber, ρ_s = the density of silica, ρ_g = density of graphene, and ρ_m = the density of matrix.

The following formula (3) [70] can be used to get the volume fraction of voids (v_v).

$$v_v = \frac{(\rho_t - \rho_a)}{\rho_t} \tag{3}$$

2.3.2 Hardness measurement

The Rockwell hardness of the CF/PA6 blend and their hybrid nanocomposites was measured on the M-scale using a Rockwell hardness tester (Saroj Engineering Udyog Pvt. Ltd., Jaysingpur, Maharashtra, India). Samples, 40 mm square plates with a 4 mm thickness, were prepared by injection molding. Testing followed ISO 2039 standards, and each data point represents the average of 10 replicates.

2.4 Characterization of the hybrid nanocomposites

2.4.1 Interlaminar shear test

The interlaminar shear strength (ILSS) of the CF/PA blend composites and their hybrid nanocomposites was determined using a JJ Lloyd EZ 20 universal testing machine, following ISO 14130. The short beam shear test employed samples with a breadth twice the thickness and a span-to-depth ratio of 4:1 (dimensions: 4 mm × 8 mm × 24 mm, span length: 16 mm). The ILSS test speed was 1 mm/min, and a 2 kN load cell was used. All reported data are averages of at least three tests.

2.4.2 Tensile and flexural testing

The tensile strength, modulus, and elongation of dumbbell-shaped CF/PA blend and their hybrid nanocomposite specimens, injection molded to ISO 527-2 type 1B dimensions were measured using a JJ Lloyd EZ 20 universal testing machine at a strain rate of 50 mm/min. According to ISO 178, 125 mm × 12.7 mm × 4 mm rectangular bars were subjected to flexural strength and modulus tests using the same universal testing machine at a strain rate of 2.5 mm/min. All reported data are averages of at least three tests.

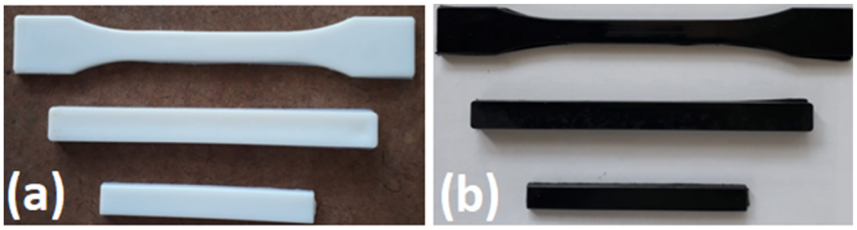

Figure 2: Photographs of the injection moulded (a) CF/PA blend composite, (b) hybrid nanocomposites.

2.4.3 Impact testing

The impact strength of the prepared CF/PA6 blend composite and their hybrid nanocomposites was tested according to ISO 180:2023 using injection-moulded rectangular bars (80 mm × 10 mm × 4 mm) with a V-shaped notch, maintaining a depth below the notch of 8 ± 0.1 mm. A CEAST-Instron pendulum impact tester with 5 J hammer energy was used for testing. All reported data are averages of at least three tests.

2.4.4 Scanning electron microscopy

The Quanta 200 model Environmental Scanning Electron Microscope (E-SEM) (FEI, Netherlands) was used to analyze the fractured surface morphology of a few selected CF/PA6 blend hybrid nanocomposites at an accelerating voltage of 20 kV. To enhance electrical conductivity and image quality, a thin layer of gold was sputter-coated onto the fracture surfaces before imaging. The obtained SEM micrographs were examined to evaluate the distribution of voids and fiber dispersion within the composite matrix, offering information on the hybrid nanocomposites' structural integrity and interfacial bonding.

3 Results and discussion

3.1 Physical properties of the hybrid nanocomposites

The densities of the H0 composite and nanofiller-reinforced hybrids (H1 to H3) are summarized in Table 2, which demonstrates a high degree of agreement between the predicted and measured values. Because of voids in the matrix caused by nanofiller aggregation, measured densities are marginally lower than theoretical ones. Nonetheless, the void content in every sample remained low at less than 1.51 %. The decreased voids in H1 to H3 might be the consequence of silane-treated nanofillers improving resin flow through processing by reducing viscosity and encouraging improved fiber wetting. Additionally, their high surface area enhances their interaction with the resin, reducing voids and facilitating its spread into fiber interfacial regions.

Table 2 shows that the density of the nanofillers modified H0 hybrid nanocomposites rose with higher filler loading (H1 to H3). Conversely, the hybrid nanocomposite with a 1.50 wt% silica loading (H2) increased the density of the H0 composite by 15.15 %. Comparing to the H0 composite, the H3 composite's density rose by 16.67 % as a result of adding mixed nanofillers (0.75 wt% silica + 0.75 wt% graphene). This density change was attributed mostly to the basic density of the nanofillers. Furthermore, PA6's density is 1.14 g cm^{-3}, lower than that of CoPe, CF, silica, and graphene. The addition of these fibres and nanofillers thereby slightly raised the density.

3.2 Rockwell hardness of the hybrid nanocomposites

The impact of loading graphene and silica nanofillers on the hardness of hybrid nanocomposites is depicted in Figure 3. Hardness rises with silica content; improvements of about 8.45 % and 14.1 % are shown by H2 (1.5 wt% silica) and H3 (1.5 wt% combined fillers), respectively. Both nanofillers improve hardness, but silica works better than graphene. H0 (without fillers) had the lowest hardness, while H3 had the highest. By improving filler–matrix adhesion, the silane-treated nanofillers' functional groups are responsible for the notable increase in hardness. The improved hardness in the hybrid composites was a result of improved bonding and dispersion.

The improved load transfer between the fiber, filler, and thermoplastic matrix under compressive force is responsible for the hybrid nanocomposites' increased hardness. Stress transfer is made more efficient by silane-treated nanoparticles' strong interfacial bonding. As demonstrated in H2, the silane treatment specifically decreases nanoparticle agglomeration, enhancing surface contact with the matrix and enhancing adhesion. Compared to H0, H2 has a higher hardness because of its superior material qualities and silica

Table 2: Density, hardness, and ILSS of CF/PA blend hybrid nanocomposites.

Sample ID	Measured density (g/cm^3)	Theoretical density (g/cm^3)	Voids (%)	Hardness (M scale)	ILSS (MPa)
H0	1.32 ± 0.01	1.34	1.51	71 ± 1	31.86 ± 1.2
H1	1.42 ± 0.02	1.44	1.41	73 ± 2	35.95 ± 1.1
H2	1.52 ± 0.02	1.54	1.30	78 ± 1	38.35 ± 1.3
H3	1.54 ± 0.01	1.56	1.28	81 ± 1	42.15 ± 1.1

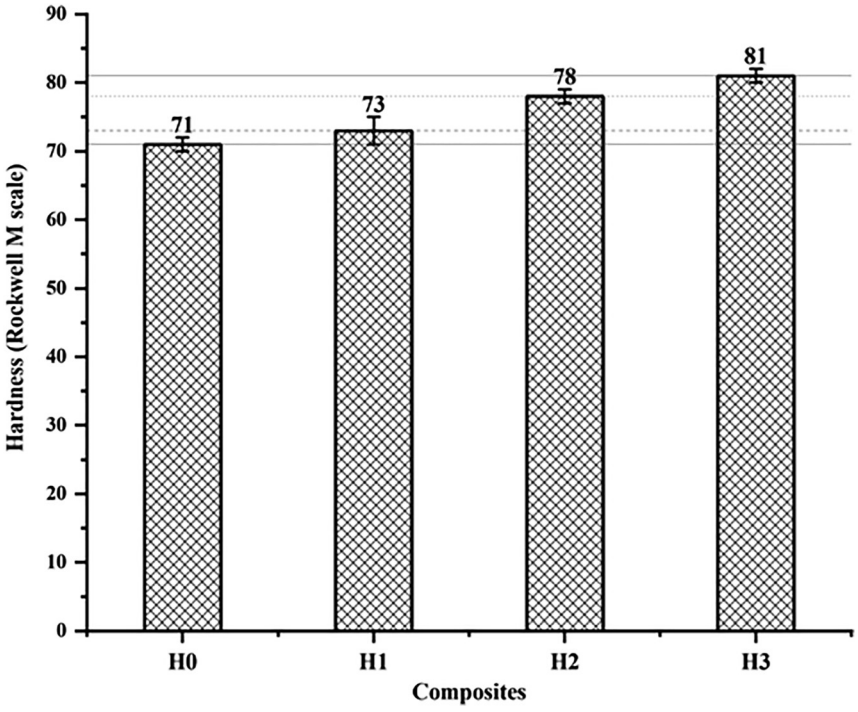

Figure 3: Influence of nanofillers loading on hardness of CF/PA blend hybrid nanocomposites.

bond. Variations in the type, size, shape, loading, and surface treatment of nanoparticles can impact bonding and result in voids. Due to strong bonding, low void content, and uniform nanofiller dispersion, H3 obtained the highest hardness value of 81, which was 14.1 % higher than H0. The synergistic impacts of clay hardness and graphene's lubricating function allowed epoxy nanocomposites with MMT and GNPs to attain better strength, stiffness, hardness, and wear resistance [71]. Similar to their thermoset epoxy system, this research highlights the advantages of dual nanofillers, although we focus on thermoplastic CF/PA hybrids where toughness and recyclability are crucial. In this instance, graphene improves ductility and fracture bridging, while silica increases stiffness and hardness, resulting in concurrent increases in tensile, flexural, and impact strength.

3.3 Interlaminar shear strength of the hybrid nanocomposites

The interlaminar shear strength (ILSS) of pure polymers is typically lower than that of fiber- and nanofiller-reinforced composites due to the absence of reinforcing structures needed to resist shear stress [72]. ILSS improves with the addition of surface-modified fibers and fillers, which reduce brittleness and enhance load transfer across the matrix. In this study, the incorporation of silane-treated silica and graphene into CF/PA6/CoPe composites significantly increased ILSS due to stronger filler–matrix bonding and improved stress transfer (Table 2).

As shown in Table 2, ILSS increased with higher silica and graphene content. Specifically, ILSS rose from 31.86 MPa in the unfilled composite (H0) to 35.95 MPa in H1 with 0.75 wt% silica, and to 38.25 MPa in H2 with 1.5 wt% silica. In H3, the hybrid composite showed a maximum ILSS improvement of 32.3 %, attributed to enhanced nanoparticle dispersion and interfacial bonding.

Silane treatment plays a key role in this enhancement by introducing functional groups (e.g., hydroxyl or amino) that improve chemical compatibility and bonding with the PA matrix. These groups facilitate covalent or hydrogen bonding, improving stress transfer and adhesion. The silane coating also reduces nanoparticle agglomeration through electrostatic repulsion, promoting uniform dispersion and minimizing stress concentrators. This resulted in better load distribution, reduced fiber pullout and void formation, and improved mechanical properties including ILSS, hardness, tensile, flexural, and impact strength.

3.4 Tensile properties of the hybrid nanocomposites

Nanofillers like silica and combined silica and graphene are used to enhance the mechanical properties of fiber-reinforced polymer composites. Understanding their dispersion and overall effect on the PA blend is essential. Figure 4a and b show how silica and graphene loading influence the tensile strength, Young's modulus, and elongation at break of H0 and

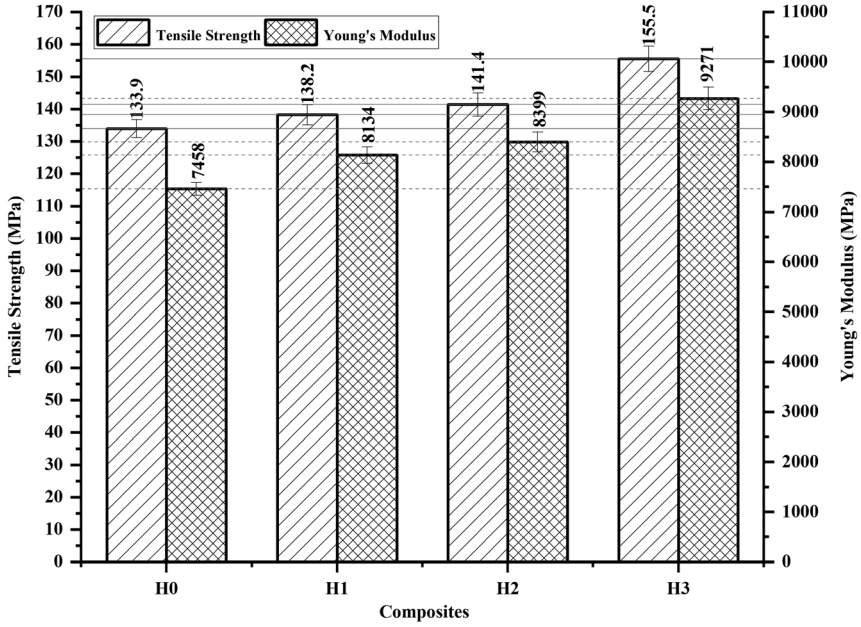

Figure 4a: Tensile properties of CF/PA blend hybrid nanocomposites.

hybrid nanocomposites (H1 to H3), with error bars indicating standard deviations.

Tensile strength increases from approximately 4.3 MPa to 21.6 MPa, and Young's modulus rises from about 676 MPa to 1813 MPa with nanofiller addition (Figure 4a). At the nanoscale, silica and graphene offer high surface area, enabling strong interaction with the polymer matrix. Graphene, known for its exceptional mechanical properties over 100 times the tensile strength of steel acts as an effective reinforcement [73]. The combined use of silica and graphene improves stiffness and strength by distributing stress more evenly across the composite, minimizing stress concentrations, and delaying failure. Enhanced surface area promotes better interfacial contact with the PA blend, while silane treatment improves adhesion, facilitating efficient stress transfer and resulting in improved tensile performance.

Figure 4a and b demonstrate how adding nanofillers to the H0 composite improves tensile strength while marginally decreasing elongation at break. This pattern holds true for hybrid nanocomposites H1 through H3. H0 has a tensile strength of 133.9 MPa and an elongation at break of 5.55 mm (Figure 4b), as shown in Figure 4a. Because of the nanofillers, H1's tensile strength is 138.2 MPa, which is 4.3 MPa higher

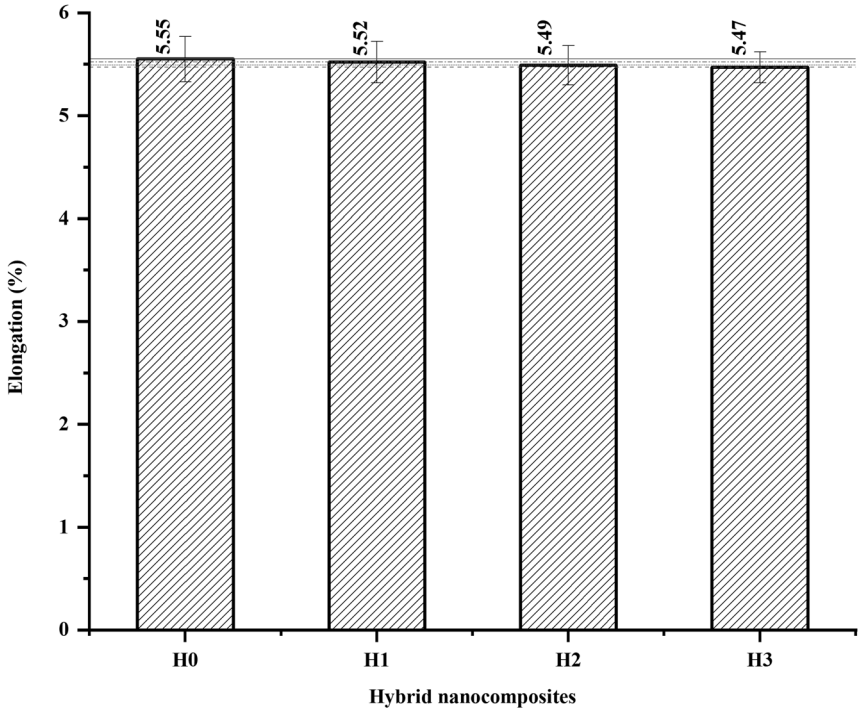

Figure 4b: Elongation at break of CF/PA blend hybrid nanocomposites.

than H0's. The addition of 1.5 wt% silica increases the stiffness of H2 by increasing its tensile strength by 7.5 MPa and its Young's modulus from 7,458 MPa to 8,199 MPa. With combined 1.5 wt% nanofiller loading, H3 shows the greatest improvement in both modulus and tensile strength. Strong interfacial adhesion between carbon fibers, nanofillers, and the PA blend matrix, as well as improved nanofiller dispersion, are responsible for these improvements.

In hybrid nanocomposites, elongation at break decreases as silica and combined silica–graphene loadings increase, as seen in Figure 4b. Because failure mechanisms have changed, similar trends have been documented in the literature [74–77]. The lower elongation at break of 14.4 % for H3 indicates that the addition of these nanofillers somewhat decreased the plastic deformation tendency of the H0 composite. H2, which contained 1.5 % silica, showed a higher elongation at break of 10.8 % compared to H3, which had a ductile failure.

Silica and graphene nanofillers make the polymer matrix more rigid and less stretchable under tensile stress by increasing its modulus and decreasing its deformability. Their interactions with the matrix, both chemical and physical, restrict the mobility of polymer chains, reducing their capacity for plastic deformation and elongation at break. The failure mode frequently changes from ductile to brittle at higher filler loadings as a result. In contrast to the filler-free H0 composite, the addition of graphene and silica in this study only slightly decreased the elongation at break (<1.5 %). The ductile behavior of the hybrid nanocomposites (H1 to H3) was maintained in spite of the increased stiffness.

Microcracks form under tensile loading at stress concentrations like fiber ends or matrix imperfections. When the applied stress exceeds local fracture toughness, these cracks propagate, weakening the material. The failure mechanism in hybrid nanocomposites depends on how microcracks interact with reinforcements like fibers and fillers. Fiber ends, as load path discontinuities, create stress concentrations that can lead to debonding or matrix fracture due to poor stress transfer (see Figure 5). Fiber alignment and aspect ratio also affect stress concentration and damage progression. Microcracks typically originate near fiber ends or defects and coalesce under continued stress.

In this study, silica particles improve matrix stiffness, toughness, and crack resistance by acting as energy dissipators and crack barriers. Stress transfer is improved by their even dispersion, which lowers stress concentrations at fiber ends. In addition to improving load transfer, graphene bridges cracks, and improves matrix ductility for better stress distribution because of its high aspect ratio and strength. Together, silica and graphene enhance load transfer and interfacial bonding; silica increases toughness, while graphene fortifies the interface. Through this synergy,

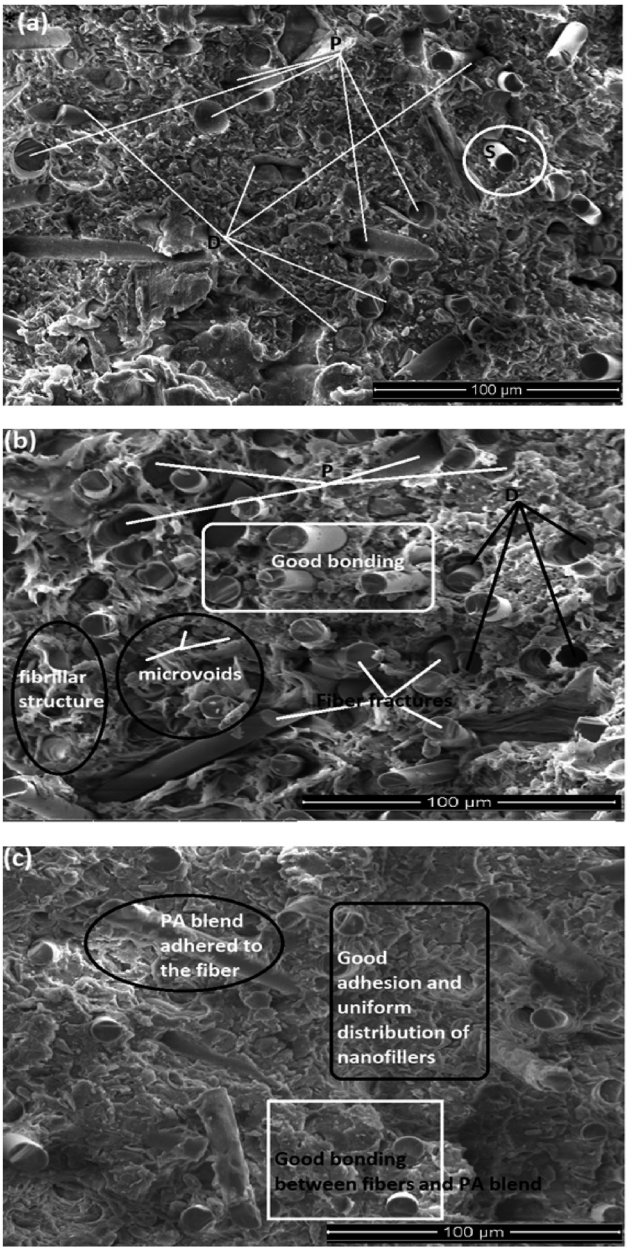

Figure 5: SEM of tensile ruptured surfaces of silica and graphene modified CF/PA blend hybrid nanocomposites: (a) H0, (b) H2, (c) H3.

crack propagation is limited, micro-crack initiation is decreased, and tensile failure resistance is increased. As a result, the H2 and H3 composites' elongation at break only dropped by 1.1 % and 1.4 %, respectively.

3.5 Fractography of tensile test failed hybrid nanocomposites

The fracture surfaces of the mono and hybrid composite tensile test samples H0, H2, and H3 are displayed in Figure 5.

The fracture surface was perpendicular to the direction of uniaxial loading. The fracture surface of samples depicted in Figure 5a–c demonstrate pull-out of fibers, fiber fracture, ductile fractures with dimples, fiber–matrix debonding and fibrillar structures.

With reference to the tensile test-failed sample H0 in Figure 5a, the H0 composite exhibits voids (zone S), interfacial debonding (zone D), and clear fiber pull-out (zone P), all of which are in agreement with the 1.51 % observed void content (Table 2). These morphological characteristics validate ineffective stress transfer and poor fiber–matrix adhesion, which restrict modulus and tensile strength. The brittle character of failure and the inferior mechanical performance of H0 can be explained by the existence of smooth fiber surfaces and gaps around fibers, which allowed the early start and propagation of cracks.

The composite with 1.5 wt% silica reinforcement exhibits fewer voids (1.3 %, Table 2) and better interfacial bonding, as demonstrated by decreased fiber pull-out and enhanced resin impregnation of the carbon fibers, according to the tensile test-failed sample H2 (Figure 5b). Visible dimples and fibrillar formations show partial energy dissipation and localized plastic deformation after failure. The observed increases in modulus and tensile strength over H0 are consistent with these microstructural characteristics. By acting as stress redistributors and crack deflectors, the silica particles increase stiffness while marginally decreasing ductility.

The hybrid composite (silica + graphene) has the best morphology and the lowest void content (1.28 %, Table 2) for the H3 sample (Figure 5c). Fractured fibers predominate over pull-out, showing good adhesion and effective stress transfer, and fibers are firmly entrenched in the PA blend. The density increase (1.54 g/cm^3 against 1.32 g/cm^3 for H0) is supported by the lack of significant voids, indicating homogeneous dispersion of the nanofiller. Since the combined reinforcing of graphene and silica limited the onset of microcracks and enhanced load-bearing capacity, these properties immediately correlate to the highest tensile strength and stiffness among the composites under study.

3.6 Flexural properties of the hybrid nanocomposites

Figure 6 shows how H0 and its hybrid nanocomposites (H1–H3) vary in terms of flexural modulus and strength. Comparing silane-treated silica and graphene nanofillers to H0, both properties were enhanced. As the silica loading increased from 0.75 wt% to 1.5 wt%, the flexural modulus of H0 rose from 8,336 MPa to 8,414 MPa and 8,534 MPa (H1 and H2 composites). This improvement most likely results from the silane-treated silica particles' improved interfacial bonding within the H0 composite, which produces high silica dispersion in H1 and H2 and excellent adhesion between CFs and the PA blend.

Remarkably, for the combined nanofiller loading (0.75 wt% silica + 0.75 wt% graphene) in the H3 composite, the flexural modulus peaked at 10,421 MPa. While prior studies have reported up to 50 % increases in flexural strength in fiber-reinforced composites with platelet-shaped nanoparticles, silica loading considerably increased the flexural strength in H1 and H2 [78, 79]. For H3 composites, the highest flexural strength and modulus were 228.6 MPa and

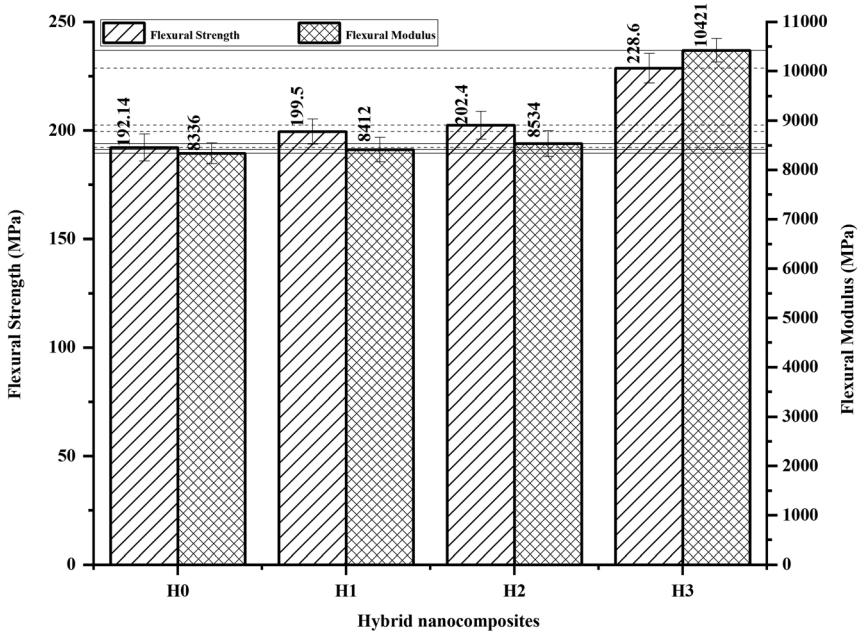

Figure 6: Flexural properties of CF/PA blend hybrid nanocomposites.

10,421 MPa, respectively. Compared to H0, this indicates a 25 % modulus and 19 % strength increase. The combined reinforcing effect of graphene and silica nanoparticles is responsible for this increase in H3, most likely as a result of the stiffening of the PA blend and the selective penetration of nanofiller into CF bundles.

Nanofillers strengthened the H0 composite and improved flexural performance by acting as load-bearers. The combined effect of silane-treated silica and graphene nanoparticles, which limit the mobility of polymer chains, is probably what caused this improvement. A previous study by Mohammed et al. [80] found that CF-reinforced epoxy containing graphene nanoplatelets and montmorillonite demonstrated enhanced flexural performance, with the latter's high loading affecting modulus. Afrouzian et al. [81] found that nano-silica improved the flexural strength of glass-reinforced epoxy. Similarly, silica nanoparticles increase the flexural modulus of polymer composites by stiffening the matrix and distributing bending stresses, according to Singh et al. [82] and Manjunath et al. [83]. The addition of graphene has also been demonstrated to greatly increase the flexural strength of laminate [84]. Graphene and silica hybrid nanofillers have a synergistic effect on flexural properties, with graphene adding ductility and strength and silica increasing stiffness, according to Mehmet et al. [85].

In the current study, graphene and silica nanofillers enhance the flexural properties of the CF/PA blend nanocomposite by fortifying the matrix. The spherical shape of silica causes it to redistribute stress and increase stiffness. Effective load transfer and crack bridging are made possible by high-strength graphene. Their combined effect enhances crack resistance and load distribution. Both fillers increase interfacial adhesion, which stiffens the matrix and facilitates better stress transfer. Whereas silica offers isotropic reinforcement, graphene offers anisotropic reinforcement. Graphene bridges cracks to stop their rapid propagation, while silica increases matrix toughness by deflecting cracks. In addition to promoting uniform stress distribution and optimizing bending performance, this combination minimizes filler agglomeration. Resistance to flexural stress is further strengthened by improved fiber–matrix adhesion. For the H3 hybrid nanocomposites, silane-treated silica and combined silica/graphene loading (≤1.5 wt%) enhanced interfacial adhesion by appropriately filling the gaps between CFs and the PA blend.

3.7 Impact strength of the hybrid nanocomposites

The impact strength of the CF/PA blend composite was enhanced by the addition of silica and graphene nanoparticles, as seen in Figure 7. In comparison to the H0 composite, the 1.5 wt% combined nanofillers (H3) produced the highest impact strength, 13.2 kJ/m^2, a 33.2 % increase. This improvement most likely comes from the nanofillers' ability to deflect fractures.

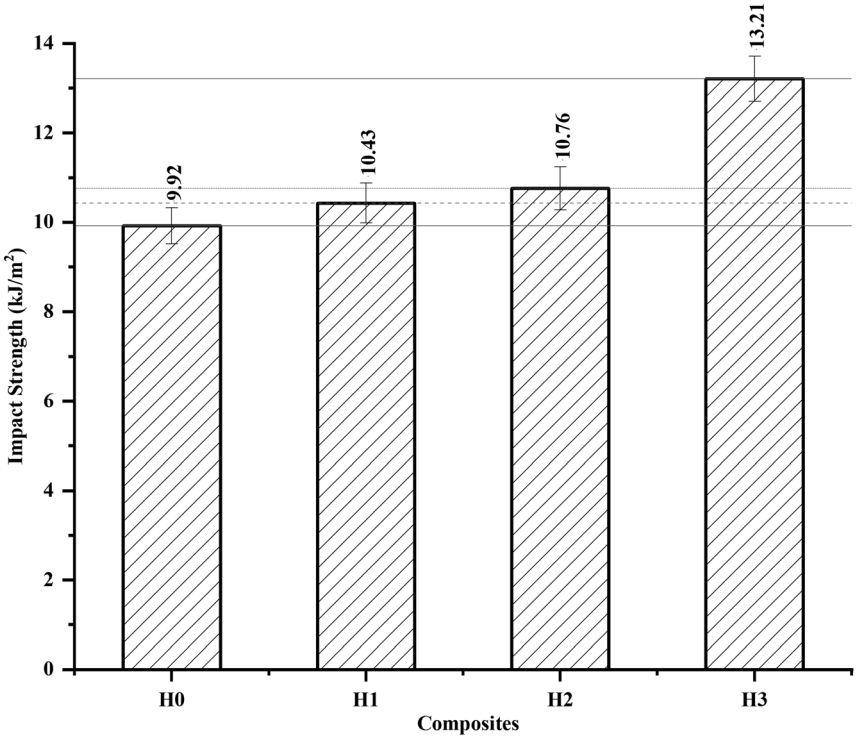

Figure 7: Impact strength of cf/PA blend hybrid nanocomposites.

Impact strength rose from 9.92 kJ/m^2 for H0 to 10.43 kJ/m^2 and 10.76 kJ/m^2 for silica-reinforced H0 blend composites (H1 and H2) at 0.75 and 1.5 wt% loadings, respectively. Silica is treated with silane and the homogeneous dispersion of nanoparticles in the H0 composite may be responsible for this improvement. In addition to discussing how interfacial adhesion affects impact strength, Kalaitzidou et al. [37] observed enhanced impact strength in PP/xGnP nanocomposites due to crack-bridging by nanoplatelets. This study, however, demonstrates a comparable toughening impact in CF/PA-based hybrids that use graphene and silica. The primary distinction is that, unlike PP systems, our dual-nanofiller method utilizes the complementing features of graphene (crack bridging) and silica (crack deflection), which together improve tensile and flexural qualities as well as impact strength.

The impact strength of H3 composite augmented with the simultaneous loading of graphene and silica. This increase can be ascribed to the H0 composite's improved nanoparticles dispersion. As a result, the fracture flow is restricted in the fiber's transverse direction. The void content may also have an impact on the impact strength values. The impact strength of the poly(arylene ether nitrile) composite has been demonstrated by Yang et al. [86] to increase even up to 20 wt% of the graphene used. The amalgamation of silica and graphene at 1.5 wt% total loading in H0 compounds can progress the impact strength up to 13.2 kJ/m^2 for H3 composite compared to H0 composite alone.

Nanoparticle accumulation in fiber and/or polymer medium compounds improves mechanical properties like intensity and stiffness. The study conducted by Landowsky et al. [87] demonstrated that the incorporation of nano-SiO_2 (up to 8 wt%) significantly reduced damage size (~28 %) and permanent deformation (~15 %) while enhancing crack branching and deflection, leading to improved fiber/matrix interfacial strength. Due to a strong correlation between fracture toughness and the particle agglomeration percolation network, the study by Lin et al. [88] found that the PA-based hybrid composite with 30 wt% silica showed the highest structural stiffness and a 45 % improvement in steady-state fracture toughness when compared to the unfilled PA. Accordingly, it is possible to improve the impact strength of fiber reinforced polymer matrix composites by combining various nanofillers. In this research work, inclusion of amalgamation of nanoparticles can pick up the diffusion of particles in the H0 compound, showing the way to enhanced impact strength. The findings are consistent with previous study by Chatterjee et al. [89] on the synergistic outcomes of hybrid nanofillers crossbreeds, such as graphene and CNTs, on the mechanical performances of epoxy compounds.

The following are the mechanisms through which silica and graphene nanofillers increase impact strength. Through processes like branching and crack deflection, silica serves as a stress redistributor, rerouting and dissipating impact energy. On the other hand, graphene can bridge cracks and stop them from growing because of its high mechanical strength and two-dimensional structure. By stretching, debonding, and encouraging localized plastic deformation, it also releases impact energy. A synergistic toughening mechanism that combines graphene and silica causes crack deflection (silica) and bridging (graphene) to occur simultaneously. Stress transfer during impact loading is improved by nanofillers, which increase the interfacial adhesion between the fiber, matrix, and nanoparticles. Better energy absorption and resistance to abrupt failure are ensured by reducing fiber pullout and void formation. Nevertheless, the inclusion of both silica and graphene nanoparticles in the present study decreased the void content (Table 2) and thereby enhanced the PA blend composite's impact strength.

3.8 Fractography of notched Izod test failed hybrid nanocomposites

Scanning electron microscopy (SEM) examined the impact fracture surfaces of CF/PA blend (H0) and its hybrid nanocomposites (H1–H3). Figure 8 shows typical SEM fracture morphology. These surfaces reveal micro-failure mechanisms including matrix cracking, interfacial debonding, fiber breakage, and fiber pull-out.

Figure 8a, which displays the fracture surface of impact test failed sample H0, demonstrates brittle failure with noticeable fiber pull-out, interfacial debonding, and crack propagation at the fiber–matrix interface. Early fracture initiation and inadequate energy absorption resulted from the increased stress concentrations caused by the larger void content (1.51 %) in H0. The lowest impact strength (9.92 kJ/m^2), where resistance to dynamic loading was limited by inadequate adhesion, is correlated with these characteristics.

Adding nanofillers like CNTs, GnPs, and TiO_2 has a big impact on how cracks spread and how stable polymer composites are. While agglomeration may serve as stress concentrators and encourage failure, uniform dispersion improves load transfer and decreases fracture initiation [90]. When properly distributed and aligned, high aspect ratio nanofillers such as CNTs and GnPs can bridge cracks and increase toughness [91]. Strong interfacial adhesion between nanofillers and the polymer matrix is essential for preventing pull-out and delamination [92], and surface functionalization can improve this even more, improving overall performance [90–92].

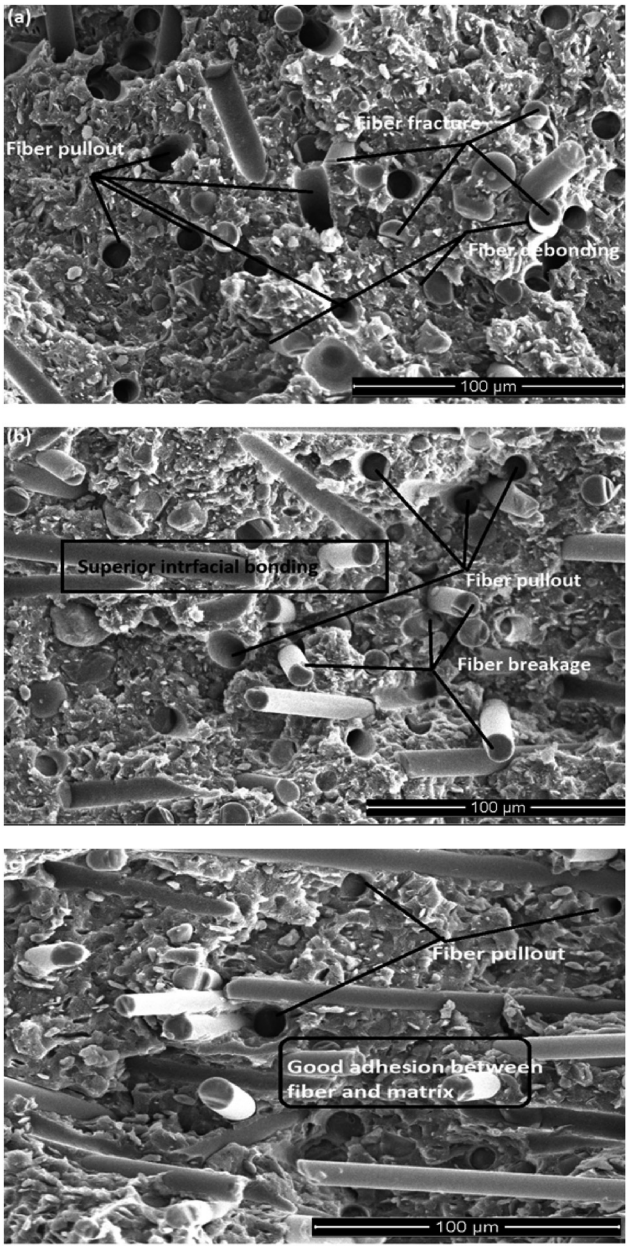

Figure 8: SEM micrographs of impact fracture surfaces of silica and graphene modified CF/PA blend hybrid nanocomposites: (a) H0, (b) H2, (c) H3.

The impact fracture surfaces of the H2 hybrid nanocomposites show a characteristic of few fibers breaking with a few fibers pull-out, as can be observed in Figure 8b. Since multiple fibers stay firmly lodged in the matrix even after fracture, the silica-filled composite shows reduced voids (1.3 %) and enhanced fiber–matrix bonding. Features of crack deflection are seen, demonstrating the function of silica in redistributing stress and releasing impact energy. The moderate increase in impact strength (10.76 kJ/m^2) over H0 is supported by these observations.

The key to the impact toughness of H3 hybrid nanocomposites is their fracture morphology. The hybrid composite exhibits the best morphology (Figure 8c), with strong fiber–matrix interlocking, minimum fiber pull-out, and few voids (1.28 %). Crack propagation is successfully inhibited, and fibers and nanofillers are firmly attached to the matrix. The homogeneous distribution of fillers, which improves interfacial adhesion and lowers flaws, is reflected in the greater density (1.54 g/cm^3). The maximum impact strength (13.2 kJ/m^2) is explained by this morphology, where the combined effects of graphene and silica allowed for simultaneous fracture bridging and deflection, promising improved energy absorption and resilience to catastrophic failure.

The correlation between SEM observations and density and void data makes it clear that increased interfacial adhesion and decreased void content are critical factors in improving impact and tensile performance. The related gains in mechanical characteristics are easily explained by the change from weak bonding and greater voids in H0 to strong interfacial linkage and reduced vacancies in H3.

3.9 Statistical analysis of mechanical properties

The mechanical properties of each composite were subjected to a one-way ANOVA and Tukey's post-hoc test in order to verify the synergistic effect of hybrid fillers (Table 3). In comparison to the unfilled (H0) and single-filler systems (H1, H2), the hybrid composite (H3) shows statistically significant improvements ($p < 0.05$) in all evaluated parameters, according to the data. For instance, ILSS increased from 31.81 ± 0.93 MPa (H0) to 42.81 ± 0.50 MPa (H3), while hardness increased from 71.30 ± 1.81 (H0) to 80.38 ± 2.04 (H3). Likewise, H3's impact strength (13.28 ± 0.33 kJ/m^2) was noticeably higher than the other composites, and its tensile and flexural strengths were much higher than those of H0–H2.

3.10 Correlation of mechanical properties

The enhancement of interfacial adhesion and stress transmission by silica and graphene nanofillers is responsible for the associated increases in hardness, tensile, flexural, and impact properties. Since the stiffer matrix prevents localized deformation and facilitates better load transfer to the fibers, the increase in hardness (14.1 % for H3) is correlated with enhanced tensile and flexural strengths. Likewise, since better interfacial adhesion lessens fiber pull-out and promotes energy dissipation through crack deflection and

Table 3: Statistical data of mechanical properties of CF/PA nanocomposites (mean ± SD, n = 5).

Property	Composite series	Mean ± SD	Significance
Hardness (Rockwell M scale)	H0	71.30 ± 1.81	a
	H1	72.26 ± 1.68	b
	H2	79.17 ± 1.62	c
	H3	80.38 ± 2.04	d
Interlaminar shear strength (MPa)	H0	31.81 ± 0.93	a
	H1	36.08 ± 1.20	b
	H2	38.36 ± 1.04	c
	H3	42.81 ± 0.50	d
Tensile strength (MPa)	H0	512.00 ± 20.74	a
	H1	551.09 ± 11.03	b
	H2	587.84 ± 17.32	c
	H3	609.29 ± 5.35	d
Flexural strength (MPa)	H0	791.65 ± 22.15	a
	H1	838.16 ± 28.06	b
	H2	875.65 ± 41.47	c
	H3	904.92 ± 25.41	d
Impact (kJ/m^2)	H0	10.04 ± 0.35	a
	H1	10.39 ± 0.35	b
	H2	10.69 ± 0.26	c
	H3	13.28 ± 0.33	D

bridging, the decrease in void content (Table 2) and stronger filler-matrix bonding not only improved ILSS but also contributed to higher impact strength (a 33.2 % increase in H3). Thus, the consistent benefits across all mechanical tests point to a single mechanism: interfacial strengthening generated by nanofiller, which simultaneously improves resistance to impact loading and static (tensile, flexural, and hardness) loading.

3.11 Industrial relevance of property improvements

For automotive and aerospace applications, where lightweight structures with high strength, toughness, and impact resistance are essential, the advancements shown in the hybrid composite (H3) are extremely pertinent. While the improved impact strength promises improved crashworthiness and damage tolerance, which are crucial for safety in the transportation sector, the notable gains in tensile and flexural strength directly support load-bearing capacity in structural components. Additionally, enhanced interfacial adhesion and decreased void content support long-term fatigue resistance, which is crucial in aerospace applications that experience cyclic loads. Together, these improvements show that the CF/PA hybrid nanocomposites not only satisfy but also closely match the mechanical performance specifications for the next generation of engineered structures that are lightweight, fuel-efficient, and damage-tolerant.

4 Conclusions

The impact of graphene and silica nanofillers on the mechanical characteristics of CF/PA blend composites was investigated in this study. The density of the CF/PA blend composite (H3) was found to be 16.67 % higher than that of the unfilled composite (H0) when small amounts of these nanofillers were added. Rockwell hardness values showed a hardening effect from the combination of graphene and silica nanoparticles, ranging from 81 (H3) to 71 (H0).

Short beam tests emphasize that silane-modified nanofillers enhance hybrid nanocomposite ILSS by improving interfacial adhesion and nanoparticle dispersion. Graphene and silica nanofillers synergistically improve CF/PA blend composite tensile strength (14.1 % in H3 vs. H0) and Young's modulus (24.3 % in H3 vs. H0). This is due to uniformly distributed nanofillers and better interfacial adhesion in the hybrid nanocomposites. Flexural strength and modulus also increased in the composite with combined 0.75 wt% silica and 0.75 wt% graphene (H3) by 16 % and 25 %, respectively, compared to CF/PA blend composite (H0).

The hybrid nanocomposite (H3) with 1.5 % nanofiller loading showed a significant 33.2 % increase in impact strength over the CF/PA blend composite (H0), outperforming the 22.8 % improvement seen with 1.5 wt% silica alone (H2).

SEM confirmed good interfacial adhesion between carbon fibers and the nanofiller-modified PA blend, facilitating effective load transfer (as visualized in SEM images) due to enhanced adhesion to silane-treated silica, graphene, and CFs. SEM micrographs also showed uniform dispersion of graphene, silica, and CFs within the PA blend. Tensile fracture surfaces in both filled and unfilled composites exhibited fiber pull-out, fiber fracture, ductile fractures with dimples, fiber–matrix debonding, and fibrillar structures.

The dual nanofiller CF/PA hybrid composites showed advantages in strength, toughness, and impact resistance that meet the performance criteria of automotive and aerospace applications for lightweight, crashworthy, and fatigue-resistant materials.

Acknowledgments: This project was funded by the Center for Research and Development of the National Institute of Engineering (NIE). The Board of Management, NIE, Principal, and Dean (Research and Development) are all appreciated by the authors. We are grateful to Mr. Byresh,

the technical specialist at the Center for Composite Materials Research, NIE, for his cooperation in carrying out the trials.
Funding information: This project was funded by the Center for Research and Development of the National Institute of Engineering (NIE).
Author contribution: All authors have accepted responsibility for the entire content of this manuscript and approved its submission.
Conflict of interest: The authors state no conflict of interest.
Data availability statement: All data generated or analysed during this study are included in this published article.

References

1. Trivedi DN, Rachchh NV. Graphene and its application in thermoplastic polymers as nano-filler-a review. Polym 2022;240:124486.
2. Sanusi OM, Benelfellah A, Hocine NA. Clays and carbon nanotubes as hybrid nanofillers in thermoplastic-based nanocomposites–A review. Appl Clay Sci 2020;185:105408.
3. Chandrasekar M, Kuma TSM, Senthilkumar K. Lightweight polymer composite structures. Boca Raton: CRC Press; 2020:309–30 pp.
4. Janarthanan P, Kumar PA, Nurazzi NM. Synthetic and natural nanofillers in polymer composites: properties and applications. United Kingdom: Elsevier Science; 2023:387–98 pp.
5. Şenyurt MA, Kurdiş MM, Ulus H, Avcı A. Enhanced mechanical and shape memory properties of Elium® nanocomposites reinforced with graphene and iron (II, III) oxide-doped polyacrylonitrile nanofibers. Fibers Polym 2025;26:2097–116.
6. Kurdiş MM, Ulus H, Avcı A. Development of innovative thermoplastic elium® nanocomposites reinforced with Ag/SiC-Doped PAN nanofibers: advancing mechanical properties and X-Ray shielding performance. Fibers Polym 2025;4:1–4.
7. Nguyen VG, Thai H, Mai DH, Tran HT, Tran DL, Vu MT. Effect of titanium dioxide on the properties of polyethylene/TiO_2 nanocomposites. Compos Part B: Eng 2013;45:192–1198.
8. Lee D, Kim S, Kim B-J, Chun SJ, Wu Q. Effect of nano-$CaCO_3$ and talc on property and weathering performance of PP composites. Int J Polym Sci 2017:1–9. https://doi.org/10.1155/2017/4512378.
9. Yuan X, Wang Y, Zhang Z, Qin R, Cao W, Zhu B. Recent advances of interfacial modifications toward carbon fiber-reinforced thermoplastic polypropylene and polyamide composites. Polym Compos 2025;46: 2911–32.
10. Sun M, Qiu Z, Chen Q, Lei H, Hua X, Zhang Z, et al. Mechanical properties of a novel mechanical metamaterial with multi-stable and mono-stable characteristics. Thin-Walled Struct 2025;212:113230.
11. Sun M, Qiu Z, Chen Q, Lei H, Zhang Z, Song Y, et al. A mechanical metamaterial for energy absorption using carbon fiber composite. Int J Mech Sci 2025;295:110282.
12. Shi T, Li KM, Wang CZ, Jin Z, Hao XK, Sun P, et al. Fracture toughness of recycled carbon fibers reinforced cement mortar and its environmental impact assessment. Case Stud Constr Mater 2025;22:e04866.
13. Yang C, Nan Z, Huo Y, Yang Y, Xu P, Xiao Y, et al. Design, characterisation, and crushing performance of hexagonal-quadrilateral lattice-filled steel/CFRP hybrid structures. Compos Part B: Eng 2025;304:112631.
14. Yao S, Chen F, Wang Y, Zhou H, Liu K. Manufacturing defect-induced multiscale weakening mechanisms in carbon fiber reinforced polymers captured by 3D CT-based machine learning and high-fidelity modeling. Compos-A Appl Sci Manuf 2025;197:109052.
15. Carothers WH; 1937. U.S. Patent, 2071253.
16. Jarovitsky PA, Maynor FL; 1972. U.S. Patent, 3681293.
17. Barnes CE; 1973. U.S. Patent, 3721652.
18. Muthuraj R, Misra M, Mohanty AK. Biodegradable compatibilized polymer blends for packaging applications: a literature review. J Appl Polym Sci 2018;135:45726.
19. Song L, Li Y, Meng X, Wang T, Shi Y, Wang Y, et al. Crystallization, structure and significantly improved mechanical properties of PLA/PPC blends compatibilized with PLA-PPC copolymers produced by reactions Initiated with TBT or TDI. Polym 2021;13:3245.
20. Alikhani E, Mohammadi M. EVA and SEBS-MA copolymers incorporated silicone rubber/SEBS blends: improvement of mechanical and thermal properties. Sci Rep 2023;13:22596.
21. Li X, He J, Hu Z, Ye X, Wang S, Zhao Y, et al. High strength carbon-fiber reinforced polyamide 6 composites additively manufactured by screw-based extrusion. Compos Sci Technol 2022;229:109707.
22. Sukia I, Esnaola A, Erice B, Aurrekoetxea J. Impact behaviour of bio-inspired sandwich panels integrally manufactured from 3D printed continuous carbon fibre reinforced polyamide. Compos Sci Technol 2024;250:110515.
23. Huang L, McCutcheon JR. Hydrophilic nylon 6, 6 nanofibers supported thin film composite membranes for engineered osmosis. J Membr Sci 2014;457:162–9.
24. Olonisakin K, Fan M, Xin-Xiang Z, Ran L, Lin W, Zhang W, et al. Key improvements in interfacial adhesion and dispersion of fibers/fillers in polymer matrix composites; focus on pla matrix composites. Compos Interfaces 2022;29:1071–120.
25. Clasen SH, Müller CM, Pires AT. Maleic anhydride as a compatibilizer and plasticizer in TPS/PLA blends. J Braz Chem Soc 2015;26:1583–90.
26. Abotbina W, Sapuan SM, Sultan MTH, Alkbir MFM, Ilyas RA. Development and characterization of cornstarch-based bioplastics packaging film using a combination of different plasticizers. Polym 2021;13:3487.
27. Kaynak C, Meyva Y. Use of maleic anhydride compatibilization to improve toughness and other properties of polylactide blended with thermoplastic elastomers. Polym Adv Technol 2014;25:1622–32.
28. Abacha N, Fellahi S. Synthesis of polypropylene-graft-maleic anhydride compatibilizer and evaluation of nylon 6/polypropylene blend properties. Polym Int 2005;54:909–16.
29. Rajak DK, Wagh Ph Linul E. Manufacturing technologies of carbon/glass fiber-reinforced polymer composites and their properties: a review. Polym 2021;13:3721.
30. Kaybal HB, Ulus H. Comparative analysis of thermoplastic and thermoset adhesives performance and the influence on failure analysis in jointed elium®-based composite structures. Polym Compos 2024; 45:3474–92.
31. Kaybal HB, Ulus H, Cacik F, Eskizeybek V, Avci A. Multi-scale mechanical behavior of liquid Elium® based thermoplastic matrix composites reinforced with different fiber types: insights from fiber–matrix adhesion interactions. Fibers Polym 2024;25:4935–50.
32. Suresha B, Hemanth G, Hemanth R, Lalla NP. Role of graphene nanoplatelets and carbon fiber on mechanical properties of PA66/thermoplastic copolyester elastomer composites. Mater Res Express 2020;7:015325.

33. Mostafa NH, Ismarrubie ZN, Sapuan SM, Sultan M. Fibre prestressed composites: theoretical and numerical modelling of unidirectional and plain-weave fibre reinforcement forms. Compos Struct 2017;159:410–23.
34. Ou Y, Zhu D, Zhang H, Huang L, Yao Y, Li G, et al. Mechanical characterization of the tensile properties of glass fiber and its reinforced polymer (GFRP) composite under varying strain rates and temperatures. Polym 2016;8:196.
35. Tesfay AG, Kahsay MB, Kumar PS. Effect of carbon and glass fillers on tensile and impact strength, water absorption, and degradation properties of sisal/polyester composites. J Nat Fibers 2023;20:2202886.
36. Ari A, Bayram A, Karahan M, Karagöz S. Comparison of the mechanical properties of chopped glass, carbon, and aramid fiber reinforced polypropylene. Polym Polym Compos 2022;30. https://doi.org/10.1177/09673911221098570.
37. Kalaitzidou K, Fukushima H, Drzal LT. Mechanical properties and morphological characterization of exfoliated graphite–polypropylene nanocomposites. Compos Part A Appl Sci Manuf 2007;38:1675–82.
38. Miao M, Wei C, Wang Y, Qian Y. Effect of compatibilizer on the interface bonding of graphene oxide/polypropylene composite fibers. Polyms 2018;10:1283.
39. Teng C-C, Ma C-CM, Huang Y-W, Yuen SM, Weng CC, Chen CH, et al. Effect of MWCNT content on rheological and dynamic mechanical properties of multiwalled carbon nanotube/polypropylene composites. Compos Part A Appl Sci Manuf 2008;39:1869–75.
40. Wu CL, Zhang MQ, Rong MZ, Friedrich K. Silica nanoparticles filled polypropylene: effects of particle surface treatment, matrix ductility and particle species on mechanical performance of the composites. Compos Sci Technol 2005;65:635–45.
41. Zheng Y, Zheng Y, Ning R. Effects of nanoparticles SiO_2 on the performance of nanocomposites. Mater Lett 2003;57:2940–4.
42. Siengchin S, Dangtungee R. Polyethylene and polypropylene hybrid composites based on nano silicon dioxide and different flax structures. J ThermoplastCompos Mater 2014;27:1428–47.
43. Radakisnin R, Abdul Majid MS, Jamir MRM, Jawaid M, Sultan MTH, Mat Tahir MF. Structural, morphological and thermal properties of cellulose nanofibers from Napier fiber (Pennisetum purpureum). Mater 2020;13:4125.
44. Fu SY, Lauke B, Mäder E. Tensile properties of short-glass-fiber- and short-carbon-fiber-reinforced polypropylene composites. Compos Part A Appl Sci Manuf 2000;31:1117–25.
45. Cho BG, Lee JE, Hwang SH, Han JH, Chae HG, Park YB. Enhancement in mechanical properties of polyamide 66-carbon fiber composites containing graphene oxide-carbon nanotube hybrid nanofillers synthesized through in situ interfacial polymerization. *Compos Part A Appl Sci Manuf* 2020;135:105938.
46. Ayyappa A, Arvydas P, Andrius V, Janusas G. Review of hybrid fiber based composites with nano particles–material properties and applications. Polyms 2020;12:2088.
47. Karnati SR, Agbo P, Zhang L. Applications of silica nanoparticles in glass/carbon fiber-reinforced epoxy nanocomposite. Compos Comm 2020;17:32–41.
48. Ma PC, Siddiqui NA, Marom G, Kim JK. Dispersion and functionalization of carbon nanotubes for polymer-based nanocomposites: a review. Compos Part A Appl Sci Manuf 2010;41:1345–67.
49. Ahmad H, Fan M, Hui D. Graphene oxide incorporated functional materials: a review. Compos Part B Eng 2018;145:270–80.
50. Fenta EW, Mebratie BA. Advancements in carbon nanotube-polymer composites: enhancing properties and applications through advanced manufacturing techniques. Heliyon 2024;10:e36490.
51. Shibuya R, Morimune-Moriya S. Reinforcement effects of graphene oxide in polyamide 6 nanocomposite system synthesized by in-situ polymerization. Polym 2024;313:127690.
52. Sabet M. Boosting polyamide 6: a comparative study on graphene and graphene oxide for improved mechanical and thermal properties. Polym Plast Technol Mater 2025;64:20–32.
53. Safdar M, Shafique MZ, Tahir MS. Thermal characterizations carbon nanotube-polymer composites. In: Handbook of Carbon Nanotubes. Cham: Springer International Publishing; 2022:1147–85 pp.
54. Li J, Tong L, Fang Z, Gu A, Xu Z. Thermal degradation behavior of multi-walled carbon nanotubes/polyamide 6 composites. Polym Degrad Stab 2006;91:2046–52.
55. Czel G, Sycheva A, Janovszky D. Effect of different fillers on thermal conductivity, tribological properties of Polyamide 6. Sci Rep 2023;13:845.
56. He J, Huang Y. Effect of silane-coupling agents on interfacial properties of CF/PI composites. J Appl Polym Sci 2007;106:2231–7.
57. Plueddemann EP. Silane coupling agents. New York: Springer; 1982.
58. Jiang D, Liu L, Zhao F, Zhang Q, Sun S, He J, et al. Improved interfacial properties of carbon fiber/unsaturated polyester composites through coating polyhedral oligomeric silsesquioxane on carbon fiber surface. Fibers Polyms 2014;15:566–73.
59. Xie Y, Hill CA, Xiao Z, Militz H, Mai C. Silane coupling agents used for natural fiber/polymer composites: a review. Compos Part A Appl Sci Manuf 2010;41:806–19.
60. Aziz T, Ullah A, Fan H, Jamil MI, Khan FU, Ullah R, et al. Recent progress in silane coupling agent with its emerging applications. J Polym Environ 2021;29:3427–43.
61. Fatemeh A, Amir HN. Recent advances in chemical surface modification of metal oxide nanoparticles with silane coupling agents: a review. Adv Colloid Interface Sci 2020;286:102298.
62. Zhang C, Tang Z, Guo B, Zhang L. Concurrently improved dispersion and interfacial interaction in rubber/nanosilica composites via efficient hydrosilane functionalization. Compos Sci Technol 2019;169:217–23.
63. Hemanth R, Suresha B, Sekar M. Physico-mechanical behaviour of thermoplastic co-polyester elastomer/polytetrafluoroethylene composite with short fibers and microfillers. J Compos Mater 2015;49:2217–29.
64. Behera K, Chang Y-H, Chiu F-C. Manufacturing poly(butylene adipate-co-terephthalate)/high density polyethylene blend-based nanocomposites with enhanced burning anti-dripping and physical properties – effects of carbon nanofillers addition. Compos Part B Eng 2021;217:1359–8368.
65. Umesh GL, Krishna Prasad NJ, Rudresh BM, Devegowda M. Influence of nano graphene on mechanical behavior of PA66/PA6 blend based hybrid nano composites: effect of micro fillers. Mater Today Proc 2020;20:228–35.
66. Üçpinar Durmaz B, Aytac A. The synergistic effects of micro-and nano-fillers on the properties of polyamide 11/poly (lactic acid) blend. J ThermoplastCompos Mater 2023. https://doi.org/10.1177/08927057231205453.
67. Liu Y, Deng Z, Zhang W, Jiang G, Cao W, Huang Z, et al. Lightweight, high-strength, heat-resistant TiB_2–B_4C-modified phenolic aerogel/carbon fiber composites with excellent thermal stability, oxidation, and ablation resistance for thermal protection. Adv Compos Hybrid Mater 2025;8:24.
68. Wang Y, Niu Z, Han H, Wang J. Observation of structural, mechanical, thermal and microwave dielectric properties of carbon black reinforced PA6/HDPE nanocomposites. J Mater Sci: Mater Electron 2023;34:1948.

69. Berti GB, Piazza D, Bortoli BF, Brandalise RN. Enhancing polypropylene composites: synergistic effects of graphene nanoplatelets and glass fibers on mechanical and thermal properties. J Nanopart Res 2024;26:154.
70. Agarwal BD, Broutman LJ. Analysis and performance of fiber composites, 2nd ed. New Jersey: John Wiley & Sons; 1990:2–16 pp.
71. Kazemi-Khasragh E, Bahari-Sambran F, Platzer C, Eslami-Farsani R. The synergistic effect of graphene nanoplatelets–montmorillonite hybrid system on tribological behavior of epoxy-based nanocomposites. Tribol Int 2020;151:106472.
72. Cheon J, Kim M. Impact resistance and interlaminar shear strength enhancement of carbon fiber reinforced thermoplastic composites by introducing MWCNT-anchored carbon fiber. Compos Part B Eng 2021; 217:108872.
73. Papageorgiou DG, Kinloch IA, Young RJ. Mechanical properties of graphene and graphene-based nanocomposites. Prog Mater Sci 2017; 90:75–127.
74. Arao Y, Yumitori S, Suzuki H, Tanaka T, Tanaka K, Katayama T. Mechanical properties of injection-molded carbon fiber/polypropylene composites hybridized with nanofillers. Compos Part A Appl Sci Manuf 2013;55:19–26.
75. Hossen MF, Hamdan S, Rahman MR, Liew FK, Lai JC. Effect of fiber treatment and nanoclay on the tensile properties of jute fiber reinforced polyethylene/clay nanocomposites. Fibers Polyms 2015;16:479–85.
76. Rasana N, Jayanarayanan K. Polypropylene/short glass fiber/nanosilica hybrid composites: evaluation of morphology, mechanical, thermal, and transport properties. Polym Bull 2018;75:2587–605.
77. Junaedi H, Baig M, Dawood A, Albahkali E, Almajid A. Mechanical and physical properties of short carbon fiber and nanofiller-reinforced polypropylene hybrid nanocomposites. Polyms 2020;12:2851.
78. Aurilia M, Sorrentino L, Sanguigno LS, Iannace S. Nanofilledpolyethersulfone as matrix for continuous glass fibers composites: mechanical properties and solvent resistance. Adv Polym Technol 2010;29:146–60.
79. Boo WJ, Sun L, Liu J, Moghbelli E, Clearfield A, Sue H, et al. Effect of nanoplatelet dispersion on mechanical behavior of polymer nanocomposites. J Polym Sci B Polym Phys 2007;45:1459–69.
80. Mohammed Z, Tcherbi-Narteh A, Jeelani S. Effect of graphene nanoplatelets and montmorillonitenanoclay on mechanical and thermal properties of polymer nanocomposites and carbon fiber reinforced composites. SN Appl Sci 2020;2:1–14.
81. Afrouzian, A, MovahhediAleni, H, Liaghat, G, Ahmadi, HLiaghatEffect of nano-particles on the tensile, flexural and perforation properties of the glass/epoxy composites. J Reinf Plast Compos 2017; 36: 900-16.DOI.
82. Singh T, Gangil B, Ranakoti L, Joshi A. Effect of silica nanoparticles on physical, mechanical, and wear properties of natural fiber reinforced polymer composites. Polym Compos 2012;42:2396–407.
83. Manjunath M, Renukappa NM, Suresha B. Influence of micro and nanofillers on mechanical properties of pultruded unidirectional glass fiber reinforced epoxy composite systems. J Compos Mater 2016;50: 1109–21.
84. Srivastava AK, Gupta V, Yerramalli CS, Singh A. Flexural strength enhancement in carbon-fiber epoxy composites through graphene nano-platelets coating on fibers. Compos Part B Eng 2019;179: 107539.
85. Mehmet VC. The synergistic effect of hybrid nano-silica and GNP additives on the flexural strength and toughening mechanisms of adhesively bonded joints. Int J Adhes Adhes 2023; 122:103333.
86. Yang X, Wang Z, Xu M, Zhao R, Liu X. Dramatic mechanical and thermal increments of thermoplastic composites by multi-scale synergetic reinforcement: carbon fiber and graphene nanoplatelets. Mater Des 2013;44:74–80.
87. Landowski M, Strugała G, Budzik M, Imielińska K. Impact damage in SiO_2 nanoparticle enhanced epoxy–Carbon fibre composites. Compos Part B Eng 2017;113:91–9.
88. Lin JC. Investigation of impact behavior of various silica-reinforced polymeric matrix nanocomposites. Compos Struct 2008;84:125–31.
89. Chatterjee S, Nafezarefi F, Tai NH, Schlagenhauf L, Nüesch F, Chu B. Size and synergy effects of nanofiller hybrids including graphene nanoplatelets and carbon nanotubes in mechanical properties of epoxy composites. Carbon 2012;50:5380–6.
90. Ramesh M, Rajeshkumar LN, Srinivasan N, Kumar DV, Balaji D. Influence of filler material on properties of fiber-reinforced polymer composites: a review. e-Polym 2022;22:898–916.
91. Yadav V, Pal D, Poonia AK. Nanofillers as a potential key for shaping the future of the industries. Hybrid Adv 2024;7:100340.
92. Ali Z, Yaqoob S, Yu J, D'Amore A. Critical review on the characterization, preparation, and enhanced mechanical, thermal, and electrical properties of carbon nanotubes and their hybrid filler polymer composites for various applications. Compos Part C Open Access 2023; 13:100434.